processes

MDPI

*Article*

# Power Spot Market Clearing Optimization Based on an Improved Low-Load Generation Cost Model of Coal-Fired Generator

**Xujia Yin [1], Hongxun Tian [2], Ce Zhou [1], Peng Zou [2], Caihuan Wu [3], Meng Qin [3] and Jun Shu [3,*]**

[1] State Grid Shanxi Electric Power Research Institute, Taiyuan 030001, China; yinxujia@yeah.net (X.Y.); happy_zc66@126.com (C.Z.)
[2] State Grid Shanxi Electric Power Company, Taiyuan 030001, China; tianhongxun2025@163.com (H.T.); zoupeng19880308@163.com (P.Z.)
[3] School of Electrical and Electronic Engineering, North China Electric Power University (Shahe Campus), Beijing 102206, China; 18170798836@163.com (C.W.); mengqin222@gmail.com (M.Q.)
* Correspondence: junshu2000@sohu.com

**Abstract**

With the rapid expansion of variable renewable energy, coal-fired units are increasingly operated at low load, where non-convex cost characteristics pose challenges for spot market clearing. This study reviews and improves existing low-load generation cost models, introducing three key enhancements: (1) integrating piecewise linearization with the marginal cost approach to reduce computational burden; (2) removing redundant binary variables and incorporating previously omitted cost components to improve clearing efficiency; and (3) developing a fuel cost model that combines quasi-fixed and marginal costs for low-load generation with firing and combustion support (FCS), enabling the joint optimization of low-load and normal operations. Applied to 6-bus and provincial systems, the proposed approach achieves speed-ups of 11.3× and 6.3× over the benchmark model (Model I) while maintaining accuracy, demonstrating both its efficiency and practical applicability.

**Keywords:** power spot market; low-load generation; cost model

check for updates

Academic Editor: Hsin-Jang Shieh

Received: 30 June 2025
Revised: 14 August 2025
Accepted: 25 August 2025
Published: 28 August 2025

**Citation:** Yin, X.; Tian, H.; Zhou, C.; Zou, P.; Wu, C.; Qin, M.; Shu, J. Power Spot Market Clearing Optimization Based on an Improved Low-Load Generation Cost Model of Coal-Fired Generator. *Processes* **2025**, *13*, 2745. https://doi.org/10.3390/pr13092745

**Copyright:** © 2025 by the authors. Licensee MDPI, Basel, Switzerland. This article is an open access article distributed under the terms and conditions of the Creative Commons Attribution (CC BY) license (https://creativecommons.org/licenses/by/4.0/).

## 1. Introduction

In recent years, the operational characteristics of power systems have been significantly transformed due to the rapid development of renewable generation. The accelerated penetration of intermittent and variable renewable energy sources, such as wind and PV power, has posed greater challenges to maintaining the balance of system power and has further highlighted the need for flexible resources in power systems [1–3]. As the traditional flexible generating resource, coal-fired generators continue to play a crucial role in providing flexibility support to power system balance in terms of their large scale of controllable capacity and mature technology [4,5].

In order to meet the need of renewable energy accommodation and system operational flexibility, coal-fired generators may need to frequently operate at low-load generation. Consequently, optimizing the low-load generation of coal-fired generators has become a key focus of current research. Studies have developed coordinated optimization models for wind–coal–CCS systems to improve low-carbon performance and economic efficiency [6], and joint modeling approaches integrating wind curtailment and low-load costs to quantify wind–thermal coordination benefits [7]. Cooperative game-based frameworks have

been used to design joint operation schemes and identify key scheduling constraints [8,9]. Multi-stage optimization models incorporating graded deep peak shaving, energy storage, and electro-thermal coupling have been proposed to enhance peak-shaving capability, reduce system costs, and improve operational flexibility [10–13].

As China's electricity spot markets evolve, the coordination of low-load generation and joint clearing process within energy markets has become one of the critical issues in spot market design. Research has proposed improved fuel cost functions and LLOAF criteria to enhance economic performance [14], evaluated deep peak-shaving retrofits using fuzzy real options [15], and established market frameworks integrating day-ahead and intraday deep peak shaving with unified clearing [16,17]. Other works have developed hydro–thermal co-optimization and multi-day rolling commitment mechanisms to improve renewable integration [18,19], and market-clearing models with cost recovery and incentive mechanisms to encourage peak shaving and renewable generation rights transfer [20,21].

During the low-load generation process, coal-fired units face the dual challenges of rising operational costs and declining economic efficiency. Low-load generation not only leads to a significant increase in unit coal consumption rate and auxiliary fuel consumption but also accelerates equipment wear and tear. Additionally, the increase in pollutant emissions under low-load operating conditions adds extra environmental costs, and these factors collectively raise the overall operational costs of coal-fired units [9,22,23]. Therefore, in order to accurately reflect the actual economic costs of coal-fired units under different levels of low-load generation to ensure the fairness of market clearing results and the reasonableness of cost allocation, and simultaneously encourage coal-fired units to participate in low-load generation, thereby improving market efficiency and promoting the absorption of renewable energy, it is essential to fully consider the low-load generation cost model of coal-fired units in the electricity spot market clearing process.

Within the low-load generation without FCS, the marginal cost of coal-fired units exhibits a monotonically increasing characteristic. This can be transformed into a stepwise increasing marginal cost curve by piecewise linearizing the secondary generation cost curve. Based on this characteristic, the electricity spot market typically uses a stepwise increasing curve to represent the normal low-load generation cost model. The market-clearing model established in this way can be formulated as a mixed-integer linear programming problem, which offers high solution efficiency. However, when the unit enters the low-load generation operation range, its generation cost curve may exhibit a discontinuous, non-convex "V-shaped" characteristic [10,22] owing to significant changes in operating conditions, which presents challenges in constructing the unit's cost model. Currently, two representative methods for low-load generation cost modeling of units have emerged in the academic community: The first method does not distinguish between the normal low-load generation stage and the low-load generation stage. Instead, it introduces 0–1 auxiliary variables and uses piecewise linearization to unify the cost curve across the entire operating range into a linear form [10]. The second method, known as the marginal cost approach, is based on the characteristic that the marginal cost of low-load generation units monotonically increases with the low-load generation energy. By introducing the unit's low-load generation energy as an independent variable, this method allows for the use of a unified stepwise increasing marginal cost model for both the low-load generation and normal stages [19–21]. As a versatile modeling method, piecewise linearization is applicable for linearizing any continuous nonlinear function and is not restricted by the monotonicity of marginal values. However, this method requires the introduction of a large number of 0–1 auxiliary variables, and since the computational efficiency of mixed-integer linear programming problems is significantly negatively correlated with the number of 0–1 variables, it may lead to a substantial decrease in the calculation efficiency of elec-

tricity spot market clearing. In contrast, the marginal cost approach offers advantages in computational efficiency, but its application is based on the prerequisite that the marginal low-load generation cost must satisfy a monotonically increasing characteristic. Furthermore, the existing low-load generation cost models based on the marginal cost approach still have shortcomings: Some model structures are overly complex [19], and improvements in accuracy are still required for certain models [20,21].

In the paper, firstly, the piecewise linearization method and the marginal cost approach are integrated in order to improve the computational efficiency of the cost model based on piecewise linearization. Secondly, the low-load generation cost model based on the marginal cost approach is improved by eliminating redundant 0–1 variables and supplementing the missing cost components; the approach increases the clearing efficiency of the power spot market without compromising computational accuracy. Thirdly, a fuel cost model combined with quasi-fixed costs and marginal costs for assisting low-load generation capability is established, which enables the joint optimization of the entire low-load generation process and regular generation dispatch. Finally, the effectiveness of the proposed mathematical model is validated using case studies of both a 6-bus test system and a provincial-level power system.

In the paper, the existing low-load generation cost models are systematically reviewed, refined, and compared in terms of model complexity. The effectiveness of the proposed mathematical model is validated through case studies on both a 6-bus test system and a provincial-level power system, and practical recommendations are provided based on the case study results. The major contributions of the paper are as follows.

1. The piecewise linearization method is combined with the marginal cost approach to address the computational inefficiency of piecewise linearization cost models. This integration maintains modeling accuracy while significantly reducing the computational burden.
2. Based on the marginal cost approach, the low-load generation cost model is improved by removing redundant binary variables and incorporating previously omitted cost components. This enhancement reduces the number of integer variables, thereby increasing the clearing efficiency of electricity spot market optimization without compromising solution precision.
3. A new fuel cost model is developed that explicitly combines quasi-fixed costs and marginal costs for coal-fired units operating under low-load generation with firing and combustion support (FCS). This formulation enables the joint optimization of the entire low-load generation process and regular generation dispatch within a unified market-clearing framework.

To further clarify the novelty and contributions of this study relative to existing work, Table 1 provides a comparative summary of the core contributions of selected references and the current work.

**Table 1.** Comparative summary of the core contributions of selected references and the current work.

| Reference | Method | Complexity | FCS | Equivalence |
|---|---|---|---|---|
| [10] | piecewise linearization | high | no | yes |
| [19] | marginal cost | moderate | no | yes |
| [20,21] | marginal cost | low | no | no |
| Proposed model | marginal cost | low | yes | yes |

## 2. A Cost Model of Low-Load Generation Adapted to Power Spot Market Clearing

The low-load generation characteristic of coal-fired generators refers to the flexible controllable capability under low generation conditions that can be achieved through the optimization of combustion control and operational strategies while ensuring safe and stable operation in order to meet the requirements of high renewable energy penetration in power systems.

Low-load generation of coal-fired generators can generally be divided into 3 stages, including normal low-load generation, low-load generation without and with firing and combustion support (FCS). The cost characteristic of coal-fired generators considering low-load generation is formulated in Equation (1) as presented in Reference [22].

$$F_{i,t}(p_{i,t}) = \begin{cases} F_{i,t}^{\mathrm{N}}(p_{i,t}), & P_{i,\min} < p_{i,t} \le P_{i,\max} \\ F_{i,t}^{\mathrm{N}}(p_{i,t}) + F_{i,t}^{\mathrm{D}}(p_{i,t}), & P_{i,\min}^{\mathrm{D}} < p_{i,t} \le P_{i,\min} \\ F_{i,t}^{\mathrm{N}}(p_{i,t}) + F_{i,t}^{\mathrm{D}}(p_{i,t}) + F_{i,t}^{\mathrm{DC}}(p_{i,t}), & P_{i,\min}^{\mathrm{DC}} < p_{i,t} \le P_{i,\min}^{\mathrm{D}} \end{cases} \quad (1)$$

The generation cost during normal low-load generation is expressed in Equation (2).

$$F_{i,t}^{\mathrm{N}}(p_{i,t}) = \alpha_i \, p_{i,t}^2 + \beta_i \, p_{i,t} + \gamma_i \quad (2)$$

As shown in Figure 1 (for simplification purposes, all variables in Figures 1–6 are presented without generator and time indices), the cost characteristic of coal-fired units formulated by Equation (1) exhibits significant discontinuous and nonlinear features, which must be linearized before being effectively incorporated into the power spot market clearing model. Without consideration of the low-load generation with FCS, the cost characteristic profile of the unit forms a continuous nonlinear function across stages of normal low-load generation and low-load generation without FCS. The minimum and maximum outputs are denoted by $P_{\min}^{\mathrm{D}}$ and $P_{\max}$, respectively. There are 2 main linearization methods for such continuous nonlinear functions: (1) the piecewise linearization method and; (2) the stepwise monotonically increasing marginal cost method. The following sections provide a comparative analysis of the mathematical models corresponding to these 2 methods and present related improvements.

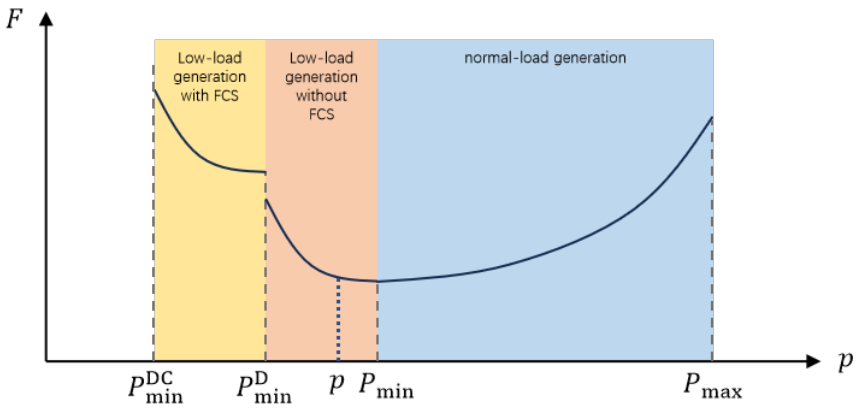



**Figure 1.** Cost characteristics of coal-fired generators.

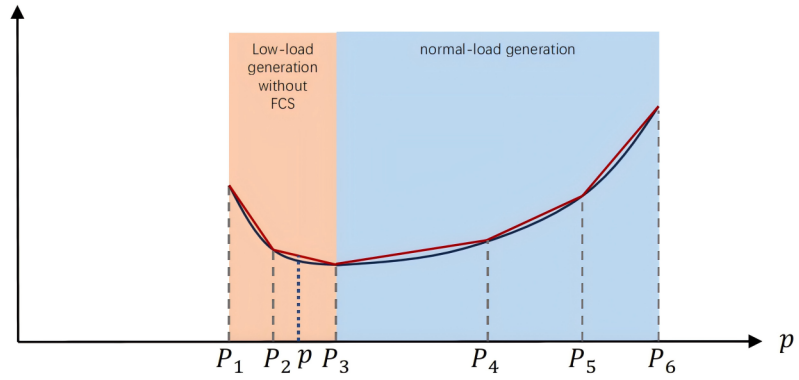



**Figure 2.** Piecewise Linearization of cost characteristics of coal-fired generators.

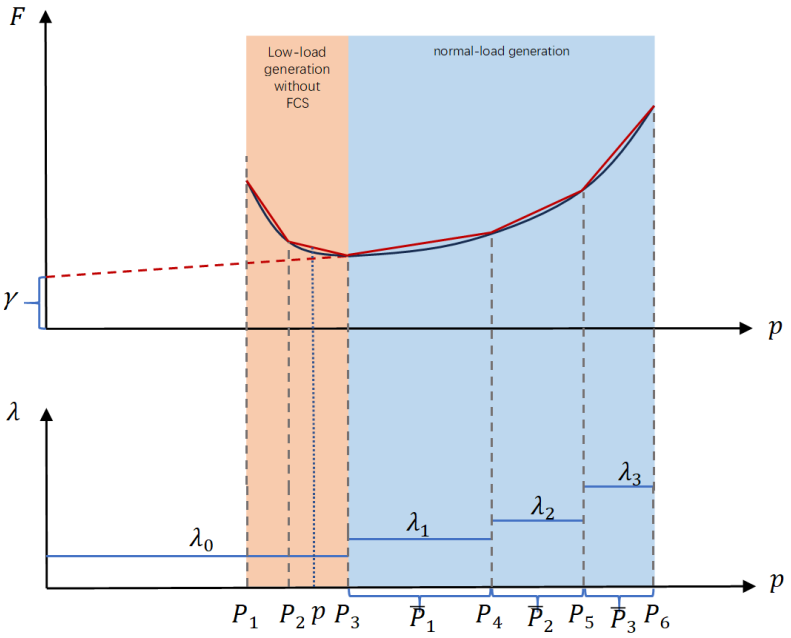



**Figure 3.** Marginal cost during normal low-load generation stage of coal-fired generators.

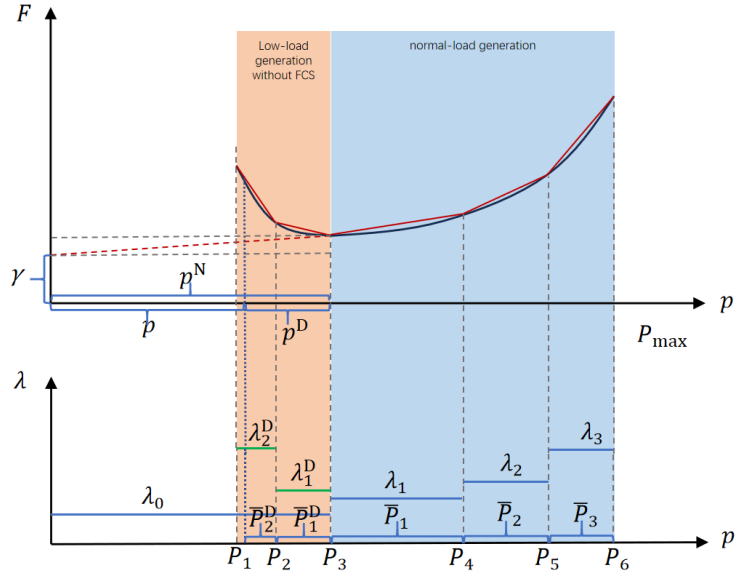



**Figure 4.** Marginal cost during stage of low-load generation without FCS of coal-fired generators.

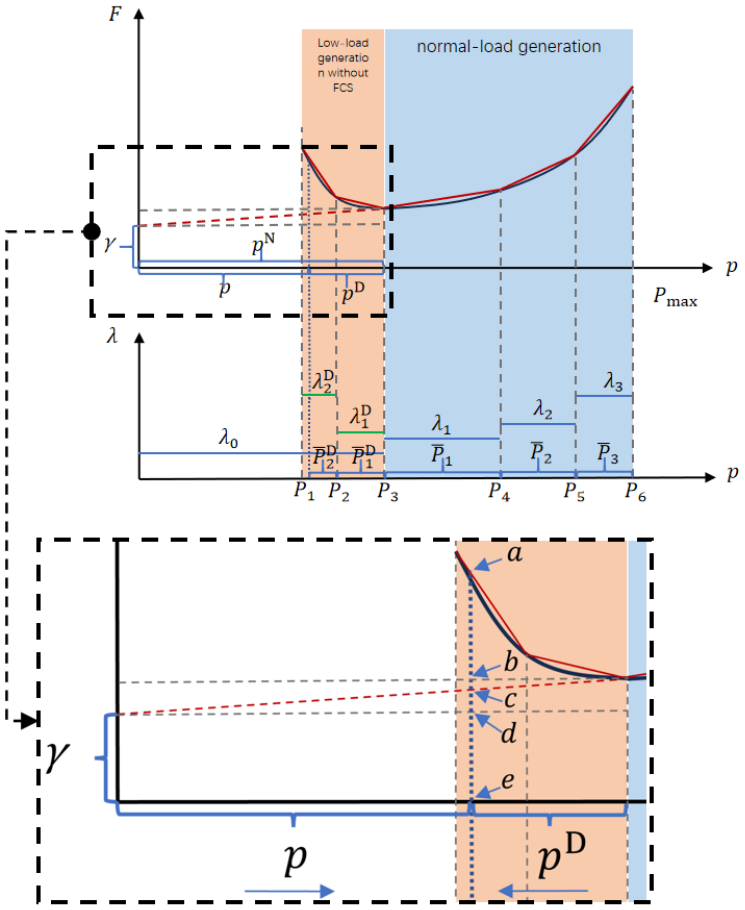



**Figure 5.** Difference between model IV and models I–III.

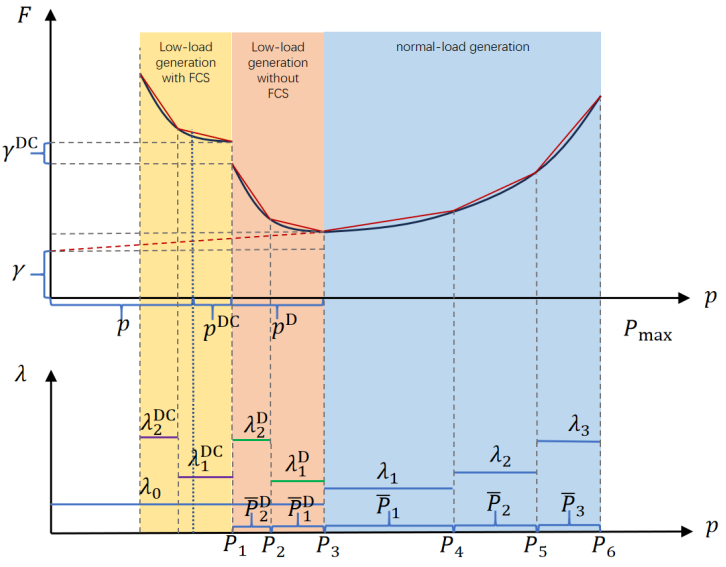



**Figure 6.** Cost characteristics of coal-fired generators considering low-load generation with FCS.

A binary auxiliary variable $d$ and a continuous auxiliary variable $e$ are introduced. The cost characteristic of any generator $i$ at any time $t$ is expressed as shown in Equation (3) [10].

$$f_{i,t} = \sum_{b=1}^{N_B+1} e_{i,b,t} F_{i,b} \Delta t, \forall i \in I^C, \forall t \tag{3}$$

### *2.1. The Piecewise Linearization Approach and Enhancement*

The piecewise linearization method is a general approach for linearizing nonlinear functions. For example, in Figure 1, the normal low-load generation stage of the generator is divided into 3 segments with $P_1^{\mathrm{N}}$ and $P_2^{\mathrm{N}}$ as the segmentation points. While the stage of the low-load generation without FCS is divided into 2 segments with $P_1^{\mathrm{ND}}$ as the segmentation point. Therefore, there are 5 linearized segments as illustrated by the red lines in Figure 2. Assuming that the cost characteristic profile is divided into $N_{\mathrm{B}}$ segments, the power values of the endpoints of the $N_{\mathrm{B}}+1$ segments are reordered in ascending order and renumbered for convenience of expression. As shown in Figure 2. The renumbered endpoints are denoted as $(P_1, F_1), (P_2, F_2), \ldots, (P_{N_{\mathrm{B}}+1}, F_{N_{\mathrm{B}}+1})$, where $P_b$ and $F_b$ represent the power and cost of the $b$-th endpoint, respectively, and $P_1 = P_{\min}^{\mathrm{D}}$, $P_{N_{\mathrm{B}}+1} = P_{\max}$. And $F_1, F_2, \ldots, F_{N_{\mathrm{B}}+1}$ represent the cost of each segment, as shown in Figure 2.

Meanwhile the following constraints should also be included

$$p_{i,t} = \sum_{b=1}^{N_{\mathrm{B}}+1} e_{i,b,t} P_{i,b}, \forall i \in I^{\mathrm{C}}, \forall t \tag{4}$$

$$e_{i,1,t} \leq d_{i,1,t}, \forall i \in I^{\mathrm{C}}, \forall t \tag{5}$$

$$e_{i,N_{\mathrm{B}}+1,t} \leq d_{i,N_{\mathrm{B}},t}, \forall i \in I^{\mathrm{C}}, \forall t \tag{6}$$

$$e_{i,b,t} \leq d_{i,b-1,t} + d_{i,b,t}, \forall i \in I^{\mathrm{C}}, \forall t, \forall b \in [2, N_{\mathrm{B}}] \tag{7}$$

$$\sum_{b=1}^{N_{\mathrm{B}}+1} e_{i,b,t} = u_{i,t}, \forall i \in I^{\mathrm{C}}, \forall t \tag{8}$$

$$\sum_{b=1}^{N_{\mathrm{B}}} d_{i,b,t} = u_{i,t}, \forall i \in I^{\mathrm{C}}, \forall t \tag{9}$$

$$e_{i,b,t} \geq 0, \forall i \in I^{\mathrm{C}}, \forall t \tag{10}$$

Equation (4) defines the relationship between the generator output and the segmentation points. Equations (5)–(7) define the relationship among the auxiliary variables. Equations (8) and (9) indicate that the generator can generate output only when it is in the operating state. Equation (8) imposes the non-negativity constraint on the auxiliary variables.

The formulation based on the piecewise linearization method as expressed in Equations (1)–(10) is referred to as Model I, in which auxiliary binary variables are introduced. And if the number of time periods is T, the number of binary variables increases by $I^{\mathrm{C}} * \mathrm{T} * N_{\mathrm{B}}$. When the number of units, time periods, and segments are relatively large, the number of binary variables increases substantially. In mixed-integer programming problem, the number of binary variables is one of the key factors determining the solving efficiency, and an excessive number of binary variables leads to a significant decline in computational performance. In addition, the introduction of the piecewise linearization method results in a large number of auxiliary constraints, which further increase the model complexity and may adversely affect the solving efficiency.

It is noteworthy that the marginal cost within the range of normal peak shaving operation of the generator exhibits a typical stepwise increasing feature, as illustrated in Figure 3. $\lambda = \frac{df}{dp}$ denotes the marginal cost of segment $\lambda$. After the cost curve in the normal peak shaving stage is linearized by the piecewise method, the resulting marginal cost profile, as shown by the blue line in the lower part of Figure 3, takes a stepwise increasing shape.

In order to reduce the number of auxiliary variables and auxiliary constraints, the normal low-load generation cost can be modeled using the marginal cost method. The stage of the low-load generation without FCS is divided into $N_B^D$ segments, and the normal low-load generation stage is divided into $N_B^N$ segments. Then $N_B^D + N_B^N = N_B$. Two binary variables, $u_{i,t}^D$ and $u_{i,t}^N$, are introduced to indicate whether generator $i$ is in the low-load generation state or the normal generation state at time $t$, respectively. The generation cost of the generator is then defined as the sum of the low-load generation cost and the normal generation cost as expressed in Equation (22).

$$f_{i,t}^D = \sum_{b=1}^{N_B^D+1} e_{i,b,t} F_{i,b} \Delta t, \forall i \in I^C, \forall t \tag{11}$$

$$p_{i,t}^D = \sum_{b=1}^{N_B^D+1} e_{i,b,t} P_{i,b}, \forall i \in I^C, \forall t \tag{12}$$

$$e_{i,1,t} \le d_{i,1,t}, \forall i \in I^C, \forall t \tag{13}$$

$$e_{i,N_B+1,t} \le d_{i,N_B,t}, \forall i \in I^C, \forall t \tag{14}$$

$$e_{i,b,t} \le d_{i,b-1,t} + d_{i,b,t}, \forall i \in I^C, \forall t, \forall b \in [2, N_B^D] \tag{15}$$

$$\sum_{b=1}^{N_B^D+1} e_{i,b,t} = u_{i,t}^D, \forall i \in I^C, \forall t \tag{16}$$

$$\sum_{b=1}^{N_B^D} d_{i,b,t} = u_{i,t}^D, \forall i \in I^C, \forall t \tag{17}$$

$$e_{i,b,t} \ge 0, \forall i \in I^C, \forall t \tag{18}$$

$$f_{i,t}^N = \left[ u_{i,t}^N (P_{i,\min} \lambda_{i,0} + \gamma_i) + \sum_{b=1}^{N_B^N} p_{i,b,t} \lambda_{i,b} \right] \Delta t, \forall i \in I^C, \forall t \tag{19}$$

$$0 \le p_{i,b,t} \le \bar{P}_{i,b,t}, \forall i \in I^C, \forall b \in N_B^N, \forall t \tag{20}$$

$$p_{i,t}^N = u_{i,t}^N P_{i,\min} + \sum_{b=1}^{N_B^N} p_{i,b,t}, \forall i \in I^C, \forall t \tag{21}$$

$$f_{i,t} = f_{i,t}^D + f_{i,t}^N, \forall i \in I^C, \forall t \tag{22}$$

$$p_{i,t} = p_{i,t}^D + p_{i,t}^N, \forall i \in I^C, \forall t \tag{23}$$

$$u_{i,t} = u_{i,t}^D + u_{i,t}^N, \forall i \in I^C, \forall t \tag{24}$$

Equation (19) defines the cost of normal-load generation for the generator. Equation (20) represents the upper and lower bounds for each normal-load generation capacity segment. Equation (21) defines the total normal-load generation output. Equation (23) indicates that the generator output equals the sum of normal-load generation and low-load generation outputs. Equation (24) represents mutual exclusivity states between the normal-load generation and low-load generation.

Equations (11)–(24) are the improved model based on the piecewise linearization method, referred to as Model II. The number of binary variables in Model II increases by $I^C * T * (N_B^D + 2)$. When $N_B^D > 2$, Model II contains fewer binary variables than Model I.

The piecewise linearization methods adopted in Models I and II are associated with inherent drawbacks, including complex expressions and low computational efficiency, and are also inconsistent with the cost model used in the normal-load generation stage

of generators. It imposes an additional cognitive burden on trading personnel in power generation companies and increases operational complexity, as well as the risk of errors in practical applications.

### 2.2. The Piecewise Linearization Approach and Enhancement

It is noted that the marginal cost during the stage of low-load generation without FCS exhibits a stepwise increasing pattern with the increase of the low-load generation $p^{\mathrm{D}}$, as shown by the red polyline in the lower part of Figure 4. In the figure, $\lambda^{\mathrm{D}}$ represents the marginal cost during low-load generation stage, $\lambda^{\mathrm{D}} = \frac{df\left(P_{\min}-p^{\mathrm{D}}\right)}{dp^{\mathrm{D}}}$. Similar to the normal-load generation stage, the marginal cost approach can be applied to model the low-load generation cost with limiting the number of 0–1 variables [19].

$$f_{i,t}^{\mathrm{D}} = \sum_{b=1}^{N_{\mathrm{B}}^{\mathrm{D}}} p_{i,b,t}^{\mathrm{D}} \lambda_{i,b}^{\mathrm{D}} \Delta t, \forall i \in I^{\mathrm{C}}, \forall t \tag{25}$$

$$p_{i,t}^{\mathrm{D}} = \sum_{b=1}^{N_{\mathrm{B}}^{\mathrm{D}}} p_{i,b,t}^{\mathrm{D}}, \forall i \in I^{\mathrm{C}}, \forall t \tag{26}$$

$$0 \le p_{i,b,t}^{\mathrm{D}} \le u_{i,t}^{\mathrm{D}} \bar{P}_{i,b,t}^{\mathrm{D}}, \forall i \in I^{\mathrm{C}}, \forall b \in N_{\mathrm{B}}^{\mathrm{D}}, \forall t \tag{27}$$

$$f_{i,t}^{\mathrm{N}} = \left[ u_{i,t}\left(P_{i,\min}\lambda_{i,0} + \gamma_i\right) + \sum_{b=1}^{N_{\mathrm{B}}^{\mathrm{N}}} p_{i,b,t}\lambda_{i,b} \right] \Delta t, \forall i \in I^{\mathrm{C}}, \forall t \tag{28}$$

$$0 \le p_{i,b,t} \le \bar{P}_{i,b,t}, \forall i \in I^{\mathrm{C}}, \forall b \in N_{\mathrm{B}}^{\mathrm{N}}, \forall t \tag{29}$$

$$p_{i,t}^{\mathrm{N}} = u_{i,t}P_{i,\min} + \sum_{b=1}^{N_{\mathrm{B}}^{\mathrm{N}}} p_{i,b,t}, \forall i \in I^{\mathrm{C}}, \forall t \tag{30}$$

$$f_{i,t} = f_{i,t}^{\mathrm{D}} + f_{i,t}^{\mathrm{N}}, \forall i \in I^{\mathrm{C}}, \forall t \tag{31}$$

$$p_{i,t} = p_{i,t}^{\mathrm{N}} - p_{i,t}^{\mathrm{D}}, \forall i \in I^{\mathrm{C}}, \forall t \tag{32}$$

$$u_{i,t}^{\mathrm{D}} \le u_{i,t}, \forall i \in I^{\mathrm{C}}, \forall t \tag{33}$$

Equation (25) defines the cost of low-load generation; Equation (26) represents the power balance for low-load generation output; Equation (27) represents the upper and lower bounds on each low-load generation segment; Equation (28) specifies the normal-load generation of the generator; Equation (31) states that the total generation cost of the generator is the sum of the low-load generation cost and the normal-load generation cost; Equation (32) indicates that the generation output is equal to the normal-load generation minus the low-load generation output, and Equation (33) ensures that low-load generation can only be performed when the generator is in operation.

Equations (25)–(33) can be referred to as Model III. This model introduces $u_{i,t}^{\mathrm{D}}$, and the number of 0–1 variables increases by $I^{\mathrm{C}} * \mathrm{T}$. However, in comparison with Model II, the total number of 0–1 variables is further reduced.

Models II and III both assume that the generator in the normal-load generation stage sets its bid from its minimum output $P_{i,\min}$. In contrast, in references [20,21], bidding starts from 0 MW and a linearized model is proposed accordingly.

$$f_{i,t}^{\mathrm{D}} = \sum_{b=1}^{N_{\mathrm{B}}^{\mathrm{D}}} p_{i,b,t}^{\mathrm{D}} \lambda_{i,b}^{\mathrm{D}} \Delta t, \forall i \in I^{\mathrm{C}}, \forall t \tag{34}$$

$$p_{i,t}^{\mathrm{D}} = \sum_{b=1}^{N_{\mathrm{B}}^{\mathrm{D}}} p_{i,b,t}^{\mathrm{D}}, \forall i \in I^{\mathrm{C}}, \forall t \tag{35}$$

$$0 \le p_{i,b,t}^{\mathrm{D}} \le \bar{P}_{i,b,t}^{\mathrm{D}}, \forall i \in I^{\mathrm{C}}, \forall b \in N_{\mathrm{B}}^{\mathrm{D}}, \forall t \tag{36}$$

$$f_{i,t}^{\mathrm{N}} = (u_{i,t}\gamma_i + \sum_{b=0}^{N_{\mathrm{B}}^{\mathrm{N}}} p_{i,b,t}\lambda_{i,b})\Delta t, \forall i \in I^{\mathrm{C}}, \forall t \tag{37}$$

$$0 \le p_{i,b,t} \le \bar{P}_{i,b,t}, \forall i \in I^{\mathrm{C}}, \forall b \in [0, N_{\mathrm{B}}^{\mathrm{N}}], \forall t \tag{38}$$

$$p_{i,t} = \sum_{b=0}^{N_{\mathrm{B}}^{\mathrm{N}}} p_{i,b,t}, \forall i \in I^{\mathrm{C}}, \forall t \tag{39}$$

$$f_{i,t} = f_{i,t}^{\mathrm{D}} + f_{i,t}^{\mathrm{N}}, \forall i \in I^{\mathrm{C}}, \forall t \tag{40}$$

$$p_{i,t} - p_{i,t}^{\mathrm{D}} \ge u_{i,t}P_{i,\min}, \forall i \in I^{\mathrm{C}}, \forall t \tag{41}$$

Equations (34)–(41) are referred to as Model IV, in which no auxiliary 0–1 variables are introduced. Model IV is a further simplified model. It should be noted that Equation (41) indicates that when the generator is in operation, the difference between its actual output and low-load generation output must be greater than or equal to the generator's technical minimum generation.

However, Model IV is not equivalent to Models I through III, which can be visually demonstrated by the enlarged view of the dashed box area in Figure 5. When the unit output is $p_{i,t}$, low-load generation output is $p_{i,b,t}^{\mathrm{D}}$, and the generation cost $f_{i,t}$ is the length of line segment $\overline{ae}$. The line segment $\overline{ae}$ can be divided into four parts; therefore, $f_{i,t} = \overline{de} + \overline{cd} + \overline{bc} + \overline{ab}$. It is clear that $\overline{de} = u_{i,t}\gamma_i\Delta t$, $\overline{cd} = \sum_{b=0}^{N_B^{\mathrm{N}}} p_{i,b,t}\lambda_{i,b}\Delta t$, $\overline{bc} = p_{i,t}^{\mathrm{D}}\lambda_{i,0}\Delta t$, $\overline{ab} = \sum_{b=1}^{N_B^{\mathrm{D}}} p_{i,b,t}^{\mathrm{D}}\lambda_{i,b}^{\mathrm{D}}\Delta t$.

However, Equations (34), (37), and (40) indicate that the generation cost $f_{i,t} = \overline{de} + \overline{cd} + \overline{ab}$ is missing $\overline{bc}$. To address this deficiency, Model IV needs to be revised by replacing Equation (34) with Equation (42).

$$f_{i,t}^{D} = \left( p_{i,t}^{D}\lambda_{i,0} + \sum_{b=1}^{N_B^{D}} p_{i,b,t}^{D}\lambda_{i,b}^{D} \right)\Delta t, \quad \forall i \in I^{C}, \forall t \tag{42}$$

Finally, Equations (35)–(42) are defined as Model V. This model is equivalent to Models I, II, and III, yet it introduces no auxiliary 0–1 variables and thus represents the most concise cost model.

Table 2 compares and summarizes the complexity of low-load generation Models I–V. Note that the number of constraints in Table 2 does not include the upper and lower bounds of variables.

**Table 2.** Complexity of low-load generation models I–V.

| Models | Number of Binary Variables | Number of Constraints |
|---|---|---|
| I | $I^c \times T \times N_B$ | $I^c \times T \times (N_B + 5)$ |
| II | $I^c \times T \times (N_B^{\mathrm{D}} + 2)$ | $I^c \times T \times (N_B^{\mathrm{D}} + 11)$ |
| III | $I^c \times T$ | $I^c \times T \times (N_B^{\mathrm{D}} + 7)$ |
| IV | 0 | $I^c \times T \times 6$ |
| V | 0 | $I^c \times T \times 6$ |

The marginal cost approach offers the advantages of concise formulation and high computational efficiency. In addition, the use of a unified cost model for both low-load generation and normal-load generation stages makes it easier for generation company traders to understand the model and prepare for the necessary data.

In addition, if the marginal cost during the low-load generation stage of certain coal-fired generators does not increase in a stepwise manner with the increase of low-load generation energy [24], Model II can be applied to those generators while Model V can be used for the others, forming a hybrid Model II+V. The hybrid model is not further discussed in the paper.

### 2.3. Cost Model for Low-Load Generation with FCS

During the stage of low-load generation with FCS, generators are required to adopt certain flame stabilization measures to enhance boiler combustion stability, such as oil injection combustion and plasma ignition technologies [9,22], which may result in a discontinuity problem in the cost function associated with the state of low-load generation with FCS, as illustrated in Figures 1 and 6. Based on Model V, a cost model referred to as Model V+ is established by introducing the 0–1 variable $u_{i,t}^{\mathrm{DC}}$, the quasi-fixed cost $\gamma_i^{\mathrm{DC}}$, and $p_{i,t}^{\mathrm{DC}}$ for low-load generation with FCS.

$$f_{i,t}^{\mathrm{D}} = (p_{i,t}^{\mathrm{D}}\lambda_{i,0} + \sum_{b=1}^{N_{\mathrm{B}}^{\mathrm{D}}} p_{i,b,t}^{\mathrm{D}}\lambda_{i,b}^{\mathrm{D}})\Delta t, \forall i \in I^{\mathrm{C}}, \forall t \tag{43}$$

$$p_{i,t}^{\mathrm{D}} = \sum_{b=1}^{N_{\mathrm{B}}^{\mathrm{D}}} p_{i,b,t}^{\mathrm{D}}, \forall i \in I^{\mathrm{C}}, \forall t \tag{44}$$

$$0 \le p_{i,b,t}^{\mathrm{D}} \le \bar{P}_{i,b,t}, \forall i \in I^{\mathrm{C}}, \forall b \in N_{\mathrm{B}}^{\mathrm{D}}, \forall t \tag{45}$$

$$f_{i,t}^{\mathrm{DC}} = (u_{i,t}^{\mathrm{DC}}\gamma_i^{\mathrm{DC}} + p_{i,t}^{\mathrm{DC}}\lambda_{i,0} + \sum_{b=1}^{N_{\mathrm{B}}^{\mathrm{DC}}} p_{i,b,t}^{\mathrm{DC}}\lambda_{i,b}^{\mathrm{DC}})\Delta t, \forall i \in I^{\mathrm{C}}, \forall t \tag{46}$$

$$p_{i,t}^{\mathrm{DC}} = \sum_{b=1}^{N_{\mathrm{B}}^{\mathrm{DC}}} p_{i,b,t}^{\mathrm{DC}}, \forall i \in I^{\mathrm{C}}, \forall t \tag{47}$$

$$0 \le \bar{p}_{i,b,t}^{\mathrm{DC}} \le u_{i,t}^{\mathrm{DC}} P_{i,b,t}^{\mathrm{DC}}, \forall i \in I^{\mathrm{C}}, \forall b \in N_{\mathrm{B}}^{\mathrm{DC}}, \forall t \tag{48}$$

$$f_{i,t}^{\mathrm{N}} = (u_{i,t}\gamma_i + \sum_{b=0}^{N_{\mathrm{B}}^{\mathrm{N}}} p_{i,b,t}\lambda_{i,b})\Delta t, \forall i \in I^{\mathrm{C}}, \forall t \tag{49}$$

$$0 \le p_{i,b,t} \le \bar{P}_{i,b}, \forall i \in I^{\mathrm{C}}, \forall b \in [0, N_{\mathrm{B}}^{\mathrm{N}}], \forall t \tag{50}$$

$$p_{i,t} = \sum_{b=0}^{N_{\mathrm{B}}^{\mathrm{N}}} p_{i,b,t}, \forall i \in I^{\mathrm{C}}, \forall t \tag{51}$$

$$f_{i,t} = f_{i,t}^{\mathrm{D}} + f_{i,t}^{\mathrm{DC}} + f_{i,t}^{\mathrm{N}}, \forall i \in I^{\mathrm{C}}, \forall t \tag{52}$$

$$p_{i,t} - p_{i,t}^{\mathrm{D}} - p_{i,t}^{\mathrm{DC}} \ge u_{i,t} P_{i,\min}, \forall i \in I^{\mathrm{C}}, \forall t \tag{53}$$

$$u_{i,t}^{\mathrm{DC}} \le u_{i,t}, \forall i \in I^{\mathrm{C}}, \forall t \tag{54}$$

Equation (46) defines the cost of low-load generation with FCS; Equation (47) represents the power balance for low-load generation output; Equation (48) indicates the upper and lower bounds for each segment of low-load generation with FCS; Equation (52) states that the generation cost of the generator is the sum of the costs from low-load generation with and without FCS to normal-load generation; Equation (53) indicates that when the

generator is in operation. The difference between its total output and the sum of the output of low-load generation without and with FCS must be greater than or equal to the generator's minimum output. Equation (54) represents that fuel-assisted low-load generation with FCS can only be performed when the generator is in operation.

## 3. Power Spot Market Clearing Model Integrated with Low-Load Generation Cost Model

With the consideration of low-load generation, the market-clearing model for the power spot market is introduced with consideration of the condition of low-load generation of coal-fired generators. The difference between the proposed model and the traditional clearing model is primarily reflected in the low-load generation cost model.

### 3.1. Objective Function

With the objective of minimizing the total system production cost as formulated in the equation.

$$\min\left(F_1 + F_2 + F_3\right) \tag{55}$$

$$F_1 = \sum_{t=1}^{\mathrm{T}} \sum_{i=1}^{I^{\mathrm{C}}} \left( y_{i,t} F_i^{ST} + f_{i,t} \right) \tag{56}$$

$$F_2 = \sum_{t=1}^{\mathrm{T}} \sum_{i=1}^{I^{\mathrm{R}}} \left( \sum_{b=0}^{N_{\mathrm{B}}^{\mathrm{N}}} p_{i,b,t} \lambda_{i,b} \right) \Delta t \tag{57}$$

$$F_3 = \rho \Delta p^{\mathrm{R}} \Delta t \tag{58}$$

$$\sum_{t=1}^{\mathrm{T}} \sum_{i=1}^{I^{\mathrm{R}}} \left[ p_{i,t} - (1-\mu) P_{i,\max} \right] + \Delta p^{\mathrm{R}} \geq 0 \tag{59}$$

### 3.2. Constraints

The clearing model is composed of generator operational constraints, energy storage operation constraints, and system operation constraints.

#### 3.2.1. Operational Constraints of Coal-Fired Generators

$$p_{i,t} + r_{i,t}^{\mathrm{U}} \leq u_{i,t} P_{i,\max}, \forall i \in I^{\mathrm{C}}, \forall t \tag{60}$$

$$p_{i,t} - r_{i,t}^{\mathrm{D}} \geq u_{i,t} P_{i,\min}^{\mathrm{DC}}, \forall i \in I^{\mathrm{C}}, \forall t \tag{61}$$

$$u_{i,t} - u_{i,t-1} = y_{i,t} - z_{i,t}, \forall i \in I^{\mathrm{C}}, \forall t \tag{62}$$

$$\sum_{t' \leq t - T_i^{\mathrm{ON}} + 1}^{t} y_{i,t'} \leq u_{i,t} z_{i,t}, \forall i \in I^{\mathrm{C}}, \forall t \tag{63}$$

$$\sum_{t' \leq t - T_i^{\mathrm{OFF}} + 1}^{t} z_{i,t'} \leq 1 - u_{i,t} z_{i,t}, \forall i \in I^{\mathrm{C}}, \forall t \tag{64}$$

$$p_{i,t-1} - p_{i,t} \leq u_{i,t} RD_i, \forall i \in I^{\mathrm{C}}, \forall t \tag{65}$$

$$p_{i,t} - p_{i,t-1} \leq u_{i,t-1} RU_i, \forall i \in I^{\mathrm{C}}, \forall t \tag{66}$$

$$r_{i,t}^{\mathrm{U}} \geq 0, \forall i \in I^{\mathrm{C}}, \forall t \tag{67}$$

$$r_{i,t}^{\mathrm{D}} \geq 0, \forall i \in I^{\mathrm{C}}, \forall t \tag{68}$$

Equation (60) represents the upper output limit constraint of the generator; Equation (61) represents the lower output limit constraint in which the minimum output limit is set to the minimum low-load generation with FCS for coal-fired generators; Equation (62) defines the coupling relationship among the generator commitment status variables; Equation (63) indicates the minimum uptime constraint; Equation (64) indicates the minimum downtime constraint; Equations (65) and (66) represent the ramp-down and ramp-up constraints, respectively; Equations (67) and (68) represent the non-negativity constraints on downward and upward reserve capacities, respectively.

3.2.2. Renewable Energy Output Constraints

$$0 \le p_{i,t} \le P_{i,\max}, \forall i \in I^{\mathrm{R}}, \forall t \tag{69}$$

$$0 \le p_{i,b,t} \le \bar{P}_{i,b}, \forall i \in I^{\mathrm{R}}, \forall b \in [0, N_{\mathrm{B}}^{\mathrm{N}}], \forall t \tag{70}$$

$$p_{i,t} = \sum_{b=0}^{N_{\mathrm{B}}^{\mathrm{N}}} p_{i,b,t}, \forall i \in I^{\mathrm{R}}, \forall t \tag{71}$$

Equation (69) represents the upper and lower bounds on the output of the renewable generation plant; Equation (70) represents the upper and lower bounds on each capacity segment of the renewable generation plant; and Equation (71) represents the power balance for the output of the renewable energy plant.

3.2.3. Operational Constraints of Energy Storage Systems

$$p_{i,t} = p_{i,t}^{\mathrm{DIS}} - p_{i,t}^{\mathrm{CHG}}, \forall i \in I^{\mathrm{S}}, \forall t \tag{72}$$

$$e_{i,t} = e_{i,t-1} + \left( p_{i,t}^{\mathrm{CHG}} \eta^{\mathrm{CHG}} - \frac{P_{i,t}^{\mathrm{DIS}}}{\eta^{\mathrm{DIS}}} \right) \Delta t, \forall i \in I^{\mathrm{S}}, \forall t \tag{73}$$

$$0 \le p_{i,t}^{\mathrm{DIS}} \le u_{i,t}^{\mathrm{DIS}} P_{i,\max}^{\mathrm{DIS}}, \forall i \in I^{\mathrm{S}}, \forall t \tag{74}$$

$$0 \le p_{i,t}^{\mathrm{CHG}} \le u_{i,t}^{\mathrm{CHG}} P_{i,\max}^{\mathrm{CHG}}, \forall i \in I^{\mathrm{S}}, \forall t \tag{75}$$

$$0 \le k_{i,t} \le K_{i,\max}, \forall i \in I^{\mathrm{S}}, \forall t \tag{76}$$

$$u_{i,t}^{\mathrm{DIS}} + u_{i,t}^{\mathrm{CHG}} \le 1, \forall i \in I^{\mathrm{S}}, \forall t \tag{77}$$

Equation (72) represents the storage power balance; Equation (73) represents the energy balance; Equations (74) and (75) specify the charging and discharging power limits, respectively; Equation (76) imposes the upper and lower bounds on the stored energy; and Equation (77) enforces the mutual exclusivity between charging and discharging.

3.2.4. System Operational Constraints

$$\sum_{i=1}^{I^{\mathrm{C}}} r_{i,t}^{\mathrm{U}} \ge RV_t^{\mathrm{U}}, \forall t \tag{78}$$

$$\sum_{i=1}^{I^{\mathrm{C}}} r_{i,t}^{\mathrm{D}} \ge RV_t^{\mathrm{D}}, \forall t \tag{79}$$

$$\sum_{i=1}^{I} p_{i,t} - \sum_{j=1}^{J} P_{j,t} = 0, \forall t \tag{80}$$

$$-H_{l,\max} \le \sum_{i=1}^{I} SF_{l,i} p_{i,t} - \sum_{j=1}^{J} SF_{l,j} p_{j,t} \le H_{l,\max}, \forall l, \forall t \quad (81)$$

Equations (78) and (79) represent the upward and downward reserve constraints of the system, respectively; Equation (80) defines the system power balance constraint; and Equation (81) represents the transmission line flow constraint.

## 4. Case Studies

The case analysis was conducted on a computer equipped with an Intel Core 6-core 2.60 GHz CPU and 16 GB of RAM, with CPLEX 22.1.1 [25] employed as the model solver.

### *4.1. 6-Bus Test System*

The one-line diagram of the 6-bus system is illustrated in Figure 7, and its basic data are provided in the Appendix A. The system consists of 6 buses, 7 transmission branches, 3 loads, 5 combined-cycle generators, 2 coal-fired generators, 1 energy storage system, 1 wind farm, and 1 PV power station. 96 time periods in a day are applied for the market clearing. It is assumed that the marginal cost of low-load generation for coal-fired generators increases in a stepwise manner as the level of low-load generation increases.

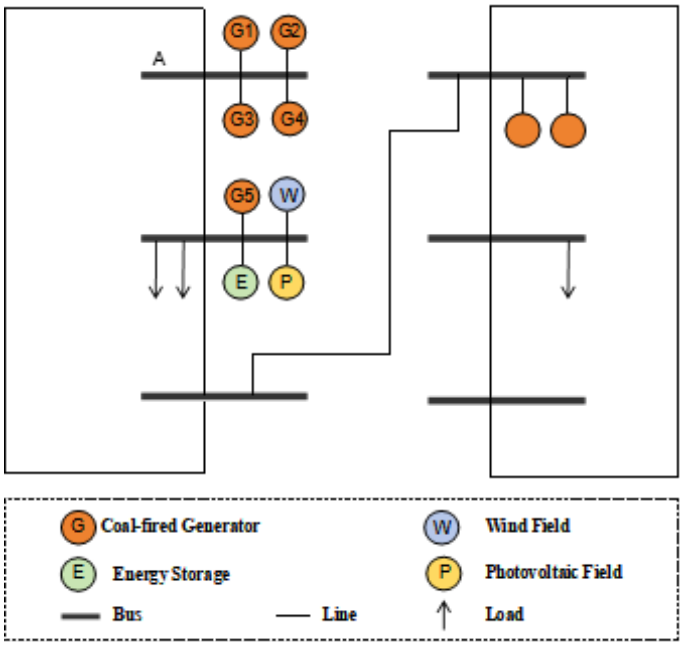



**Figure 7.** Power System Operation Analysis.

#### 4.1.1. Power System Operation Analysis

Six scenarios are designed in this study, as shown in Table 3, to analyze the impact of energy storage and low-load generation without and with FCS on system operation.

**Table 3.** Scenario settings for the 6-bus system.

| Scenario | Energy Storage | Low-Load Gen Without FCS | Low-Load Gen with FCS |
|---|---|---|---|
| 1 | No | No | No |
| 2 | No | Yes | No |
| 3 | No | Yes | Yes |
| 4 | Yes | No | No |
| 5 | Yes | Yes | No |
| 6 | Yes | Yes | Yes |

For the 6 scenarios, the system operational indices (including the renewable generation curtailment rate, system production cost, and number of generator with startups) are presented in Table 4.

**Table 4.** System operation indices for 6-bus scenarios.

| Scenario | Renewable Generation Curtailment Rate (%) | System Operating Cost (RMB) | Number of Generators with Startups |
|---|---|---|---|
| 1 | 0.12 | 9,078,464.69 | 5 |
| 2 | 0 | 7,293,477.12 | 4 |
| 3 | 0 | 7,052,133.20 | 3 |
| 4 | 0 | 7,050,739.65 | 3 |
| 5 | 0 | 6,768,059.07 | 2 |
| 6 | 0 | 6,768,059.07 | 2 |

As shown in Table 4, in Scenario 1, coal-fired generators are not capable of performing low-load generation, and energy storage is not operated; the system exhibits limited flexibility and power controllability. It results in an inability to fully accommodate renewable energy and requires frequent startups and shutdowns of coal-fired generators to provide the necessary flexibility with high system operational costs. In Scenario 2, although energy storage is not operated low-load generation without FCS by coal-fired generators is enabled, which provides a certain level of flexibility to allow full accommodation of renewable energy and reduce the number of generators with startups to 4. As a result, system operational costs are significantly reduced. In comparison with Scenario 2, in Scenario 3, low-load generation with FCS is allowed, which further enhances system flexibility to reduce the number of generators with startups to 3 and further decrease system operational costs. In contrast to Scenario 3, in Scenario 4, low-load generation for coal-fired generators is disabled and the operation of energy storage is enabled, which maintains the number of generators with startups at 3. It achieves a lower operational cost due to the relatively large capacity of energy storage and its bidirectional power controllability. In Scenario 5, both energy storage systems are operated, and low-load generation with FCS is enabled for coal-fired generators, which leads to a significant reduction in system operational costs in comparison with Scenario 4 and a decrease in the number of generators with startups to 2. In Scenario 6, although low-load generation with FCS is enabled, and low-load generation capability is not utilized because of its relatively high associated cost. It results in identical dispatch outcomes to those in Scenario 5. Table 5 shows that low-load operation of coal-fired units can enhance renewable energy integration, reduce startup frequency of coal units, and lower system operating costs. It is recommended that market designers provide coal-fired units with the opportunity to bid their low-load operating costs, thereby incentivizing them to voluntarily enhance their flexible regulation capability.

**Table 5.** Performance indices of different models in the 6-bus system.

| Model | Computational Error/% | Number of 0–1 Variables | Number of Constraints | Computation Time/s |
|---|---|---|---|---|
| I | 0 | 13,440 | 29,394 | 45 |
| II | 0 | 8064 | 23,428 | 12 |
| III | 0 | 2688 | 20,644 | 5 |
| IV | 0.61 | 2016 | 18,436 | 4 |
| V | 0 | 2016 | 18,436 | 4 |

Under market conditions, the effectiveness of low-load generation of coal-fired generators in facilitating renewable energy integration largely depends on the bidding prices of

renewable energy. Assuming that energy storage is not operated, the renewable energy curtailment rate and the amount of low-load generation under different renewable energy bidding levels are illustrated in Figure 8.

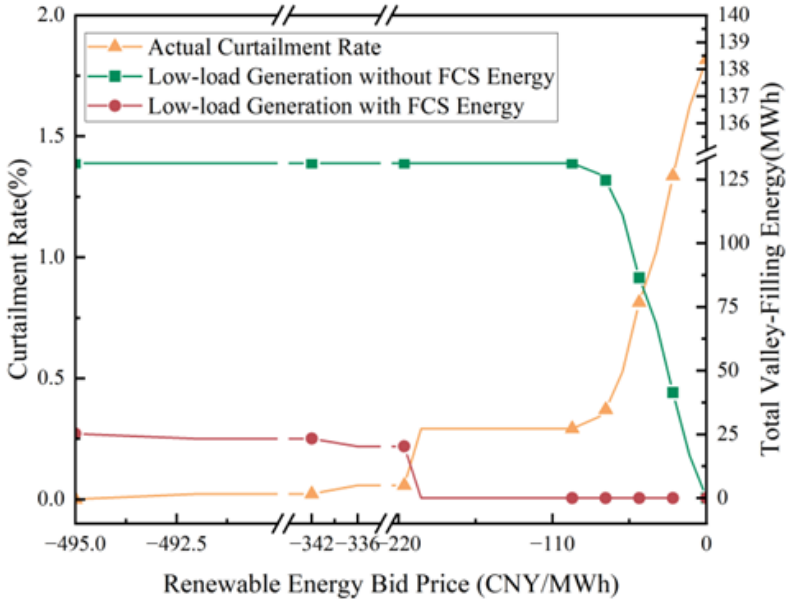



**Figure 8.** Relationship between renewable energy bidding levels, renewable curtailment rate, and low-load generation in the 6-bus system.

As illustrated in Figure 8, because the cost of the stepwise marginal cost model of low-load generation for coal-fired generators increases along with lowering output during the stage of low-load generation. Therefore, only when the bidding price of renewable generation is negative and the low-load generation cost is fully covered can coal-fired generators be incentivized to perform low-load generation to facilitate renewable generation accommodation. Since the bid price of coal-fired generators in the low-load generation stage increases in a stepwise manner, when the renewable energy bidding price decreases from −10 CNY/MWh to −75 CNY/MWh, the output of low-load generation without FCS of coal-fired generators increases. It leads to a corresponding reduction in the renewable energy curtailment rate. When the renewable energy bidding price reaches −75 CNY/MWh, the output of low-load generation without FCS reaches its maximum, and the output of low-load generation with FCS remains at 0 MWh. Since the cost of low-load generation with FCS includes no-load costs, when the renewable energy bidding price range is from −75 CNY/MWh to −204 CNY/MWh, the cost cannot be covered, and thus the output of the low-load generation with FCS still remains at 0 MWh. When the renewable energy bidding price falls below −204 CNY/MWh, the output of low-load generation with FCS begins to increase gradually with further price reductions, and the renewable energy curtailment rate continues to decline. When the bidding price reaches −495 CNY/MWh, the renewable curtailment rate drops to zero. Therefore, it is recommended that market designers set a lower market bid floor to fully incentivize coal-fired units to participate in low-load operation.

#### 4.1.2. Performance Analysis of Model Solving

The formulations of Models I–V are different, and their solution performance also varies. When energy storage is not in operation in the 6-bus system, the computational error, model scale, and computation time of Models I–V are summarized in Table 5.

In Table 5, the computational error is calculated according to Equation (82).

$$\Delta F_{\vartheta} = \frac{|F_{\vartheta} - F_I|}{|F_I|} \times 100\%, \forall \vartheta \in [II, V] \tag{82}$$

In the equation, $F_I$ represents the operating cost of Model I, and $F_{\vartheta}$ denotes the operating cost of the other models excluding Model I.

As shown in Table 5, Model I contains the largest number of 0–1 variables and constraints, which leads to the longest computation time of 45 seconds. Since Model II adopts the marginal cost approach for modeling the normal-load generation stage, both the number of 0–1 variables and constraints are significantly reduced, and the computation time decreases to 12 s. Models III to V employ the marginal cost approach, which further improves computational efficiency. Model III still introduces auxiliary 0–1 variables and remains relatively complex and achieves a computation time of 5 seconds. Model IV eliminates all 0–1 variables and achieves high computational efficiency, although a deviation of 0.62% is observed. Model V is the most concise and incurs no deviation while achieving the highest computational efficiency, which equals that of Model IV. Therefore, it is recommended that market designers adopt a market-clearing model based on Model V.

### *4.2. A Case Study of a Real Provincial-Level Power System*

The provincial-level power system consists of 5000+ buses, 6000+ transmission branches, 200+ loads, 100+ coal-fired units, 15 gas-fired units, 6 energy storage systems, 200+ wind power plant, and 100+ PV power stations. In a typical day, the system reaches a maximum load of 30,061 MW, and the maximum power of wind and PV generation are 10,014 MW and 10,927 MW, respectively. The load and renewable generation profiles are illustrated in Figure 9. The low-load generation cost data of coal-fired units (e.g., the number of low-load segments, FCS triggering conditions) used in this study are hypothetical and were assumed for the purpose of model illustration rather than obtained from actual measurements. Other parameters of this system (e.g., capacity, efficiency, ramp rates of coal-fired units) are derived from actual provincial power system data. However, due to confidentiality agreements with the data provider, the detailed values cannot be disclosed.

Similar to the 6-bus system case, 6 scenarios are also defined in this case study, as shown in Table 3. The system operational indices under these 6 scenarios, including renewable generation curtailment rate, operating cost, and the number of generators with startups, are presented in Table 6.

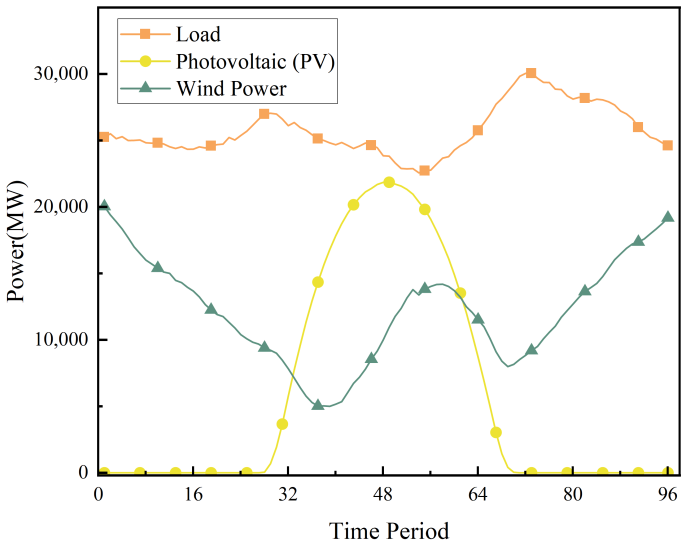



**Figure 9.** Load and renewable energy profiles of the provincial power system.

**Table 6.** System operation indicators for the provincial power system.

| Scenario | Curtailment Rate (%) | System Operating Cost (Million CNY) | Number of Generators with Startups |
|---|---|---|---|
| 1 | 5.92 | 201.77 | 58 |
| 2 | 5.20 | 196.26 | 59 |
| 3 | 5.66 | 193.80 | 51 |
| 4 | 4.06 | 179.07 | 50 |
| 5 | 3.98 | 175.41 | 46 |
| 6 | 4.20 | 174.72 | 43 |

As shown in Table 6, in comparison with the scenarios without energy storage operation, all system operational indices are improved when energy storage is in operation. This is primarily because the power controllability provided by the storage units in this case study significantly exceeds the total low-load generation capacity. Moreover, under the same energy storage operation condition, an enhancement of the low-load generation capability of coal-fired units leads to a reduction in system operating cost. The renewable generation curtailment rate and the number of generators with startups also tend to decrease accordingly. However, conflicts may occasionally arise between the renewable curtailment rate and the number of generators with startups. For example, in comparison with Scenario 1, Scenario 2 achieves a 0.72% reduction in the renewable generation curtailment rate but with 1 additional unit with startup. In contrast, in comparison with Scenario 2, Scenario 3 shows a 0.46% increase in renewable curtailment rate with a reduction in the number of generators with startups by 8. This is because coal-fired units are required to increase shutdowns during net load periods to facilitate renewable energy accommodation, which may consequently necessitate the startups of additional units during net load peak periods to meet load demand. Conversely, the opposite situation may also occur. In the absence of energy storage system operation, the performance of Models I to V is evaluated in this case study. Key performance indices, including calculation error, model scale, and computation time, are summarized in Table 7.

**Table 7.** Performance indicators of different models in the provincial power system.

| Model | Computational Error/% | Number of 0–1 Variables | Number of Constraints | Computation Time/s |
|---|---|---|---|---|
| I | 0 | 203,424 | 758,612 | 1244 |
| II | 0 | 65,376 | 612,596 | 687 |
| III | 0 | 45,408 | 437,972 | 223 |
| IV | 0.37 | 42,912 | 363,764 | 195 |
| V | 0 | 42,912 | 363,764 | 196 |

Based on the simulation results presented in Table 7, the same conclusion as well as for the 6-bus system can be drawn for the provincial-level power system case: the proposed improved Model V achieves superior computational efficiency in comparison with the other benchmark models while maintaining acceptable solution accuracy. Therefore, the effectiveness and applicability of the model are validated.

## 5. Conclusions

In this study an improved cost model of low-load generation of a coal-fired generator is proposed. Cost formulation for low-load generation with FCS composed of quasi-fixed

costs and marginal costs is established, which enables the joint optimization of the entire process of operation for low-load generation and market clearing. Based on case study analysis, the following main conclusions are drawn:

1. Based on the enhancement of the low-load generation capability of coal-fired generators and the integration of energy storage systems, a decreasing trend in system operational costs was observed. It generally facilitates renewable energy accommodation and reduces the number of generator startups. It is proposed to allow coal-fired units to bid low-load operation costs to incentivize voluntary flexibility enhancement.
2. Both low-load generation with and without FCS can effectively enhance the level of renewable energy accommodation. However, low-load generation with FCS incurs higher operational costs. Under a market-based mechanism, renewable generation producers must provide greater economic compensation to incentivize coal-fired generators to offer services of low-load generation with FCS. It is recommended to appropriately lower the price floor to create incentive conditions that encourage coal-fired units to further reduce their minimum stable generation load.
3. In comparison with existing cost models of low-load generation, the improved cost model proposed in this study demonstrates advantages in terms of model complexity, exhibiting the smallest size of optimization problem and the highest computational efficiency. It is recommended to construct the market clearing model based on Model V to the greatest extent possible.

It should be noted that certain limitations remain in applying the proposed method to China's spot markets. First, low-load generation involves multiple implicit costs that are difficult to measure accurately, and the conclusions reported in related literature are often inconsistent or disputed. Second, allowing coal-fired units to bid low-load generation costs may create opportunities for these units to exercise market power, thereby increasing the difficulty of market monitoring and regulation. Finally, since the marginal cost of low-load generation for some units may not be strictly monotonically increasing, it may be appropriate in such cases to adopt a hybrid Model II + V approach in the market clearing model.

This study assumes that the technical constraints of coal-fired units during low-load operation are identical to those under normal operating conditions. In practical applications, low-load operation may exhibit distinct technical characteristics that require alternative constraint formulations. Future research will incorporate these specific characteristics into the modeling framework to improve the model's accuracy and practical applicability.

**Author Contributions:** Conceptualization, J.S.; methodology, J.S.; software, J.S.; validation, J.S.; formal analysis, J.S.; resources, X.Y., H.T., C.Z. and P.Z.; data curation, C.W.; writing—original draft preparation, J.S.; writing—review and editing, C.W. and M.Q.; supervision, X.Y.; project administration, X.Y. and C.W.; funding acquisition, X.Y., H.T., C.Z. and P.Z. All authors have read and agreed to the published version of the manuscript.

**Funding:** This research was funded by State Grid Corporation of China Science and Technology Project "Research and application of key technologies for supporting market mechanisms to improve the regulation capabilities of power grid source and load under the conditions of energy transformation in multi coal-fired power areas (5108-202415059A-1-1-ZN)".

**Data Availability Statement:** The original contributions presented in this study are included in the article. Further inquiries can be directed to the corresponding author.

**Conflicts of Interest:** Author Xujia Yin and Ce Zhou was employed by the State Grid Shanxi Electric Power Research Institute. Author Hongxun Tian and Peng Zou was employed by the State Grid Shanxi Electric Power Company. The remaining authors declare that the research was conducted in the absence of any commercial or financial relationships that could be construed as a potential

conflict of interest. The State Grid Corporation of China Science and Technology Project had no role in the design of the study; in the analyses, or interpretation of data; in the writing of the manuscript, or in the decision to publish the results.

## Nomenclature

**Indices**

| | |
|---|---|
| $i$ | Index for coal-fired units, renewable energy plants, and energy storage systems. |
| $t$ | Index for time periods. |
| $b$ | Index for cost or capacity segments in piecewise linearization. |
| $l$ | Index for transmission lines. |
| $j$ | Indices for loads. |

**Sets and Matrices**

| | |
|---|---|
| $I^C$ | Set of coal-fired units. |
| $I^R$ | Set of renewable energy plants. |
| $I^S$ | Set of energy storage systems. |
| $I$ | Set of all generation units. |
| $J$ | Set of loads. |
| $T$ | Set of time periods. |
| $N_B$ | Total number of segments in piecewise linearization of cost curves. |
| $N_B^D$ | Number of segments for low-load generation without FCS. |
| $N_B^N$ | Number of segments for normal load generation. |
| $N_B^{DC}$ | Number of segments for low-load generation with FCS. |

**Parameters**

| | |
|---|---|
| $F_{i,t}$ | Generation cost of unit $i$ at time $t$ ($). |
| $F_{i,t}^N$ | Generation cost during normal low-load generation ($). |
| $F_{i,t}^D$ | Additional generation cost during low-load generation without FCS ($). |
| $F_{i,t}^{DC}$ | Additional generation cost during low-load generation with FCS ($). |
| $F_1$ | Generation cost of coal-fired generator including start-up cost ($). |
| $F_2$ | Cost of renewable energy ($). |
| $F_3$ | Cost of renewable energy curtailment ($). |
| $F_\theta$ | Operating cost of the other models excluding Model I ($). |
| $P_{i,\max}$ | Maximum output of unit $i$ (MW). |
| $P_{i,\min}$ | Minimum output of unit $i$ (MW). |
| $P_{i,\min}^D$ | Minimum output during low-load generation without FCS for unit $i$ (MW). |
| $P_{i,\min}^{DC}$ | Minimum output during low-load generation with FCS for unit $i$ (MW). |
| $\overline{P}_{i,b,t}$ | Upper bound of power of segment $b$ for unit $i$ at time $t$ (MW). |
| $\overline{P}_{i,b,t}^D$ | Upper bound of power of segment $b$ for unit $i$ at time $t$ during low-load generation without FCS (MW). |
| $\overline{P}_{i,b,t}^{DC}$ | Upper bound of power of segment $b$ for unit $i$ at time $t$ during low-load generation with FCS (MW). |
| $p_{i,\max}^{DIS}$ | Maximum discharging power of storage unit $i$ (MW). |
| $p_{i,\max}^{CHG}$ | Maximum charging power of storage unit $i$ (MW). |
| $K_{i,\max}$ | Maximum energy capacity of storage unit $i$ (MW). |
| $T_i^{on}$ | Minimum up time of unit $i$. |
| $T_i^{off}$ | Minimum down time of unit $i$. |
| $\Delta t$ | Duration of time period $t$. |
| $R_{i,t}^{up}$ | Upward reserve capacities of generator $i$ at time $t$. |
| $R_{i,t}^{down}$ | Downward reserve capacities of generator $i$ at time $t$. |
| $RD_i$ | Ramp-down rates of generator $i$ (MW/min). |
| $RU_i$ | Ramp-up rates of generator $i$ (MW/min). |

| | |
|---|---|
| $RV_t^U$ | Upward reserve requirements at time $t$ (MW). |
| $RV_t^D$ | Downward reserve requirements at time $t$ (MW). |
| $H_{l,\max}$ | Maximum power flow capacity of line $l$ (MW). |
| $SF_{i,l}$ | Shift factor of generation unit $i$ on line $l$. |
| $SF_{l,j}$ | Shift factor of load $j$ on line $l$. |
| $\alpha_i/\beta_i/\gamma_i$ | Cost parameters of unit $i$. |
| $Y_i^{DC}$ | Quasi-fixed cost during low-load generation with FCS. |
| $\mu$ | Maximum allowable rate of renewable generation curtailment. |
| $\lambda_{i,b}$ | Marginal cost of unit $i$ of segment $b$ during normal-load generation ($). |
| $\lambda_{i,b}^D$ | Marginal cost of unit $i$ of segment $b$ during low-load generation without FCS ($). |
| $\lambda_{i,b}^{DC}$ | Marginal cost of unit $i$ of segment $b$ during low-load generation with FCS ($). |
| $F_i^{ST}$ | Startup cost of unit $i$ ($). |
| $\rho$ | Cost of renewable energy curtailment ($). |
| $\Delta p^R$ | Represents curtailed power of renewable generation (MW). |
| $\eta^{DIS}$ | Discharging efficiency of storage unit $i$. |
| $\eta^{CHG}$ | Charging efficiency of storage unit $i$. |

**Variables**

| | |
|---|---|
| $a_{i,b,t}$ | Binary variable equal to 1 if the unit output is within segment $b$, 0 otherwise. |
| $e_{i,b,t}$ | Position of the unit output within segment $b$. |
| $k_{i,t}$ | Stored energy of storage unit $i$ at time $t$ (MW). |
| $u_{i,t}$ | Operation status variable of unit $i$ at time $t$. |
| $u_{i,t}^D$ | Indicate unit $i$ is in the low-load generation without FCS at time $t$. |
| $u_{i,t}^N$ | Indicate unit $i$ is in the normal generation state at time $t$. |
| $u_{i,t}^{DC}$ | Indicate unit $i$ is in the low-load generation with FCS at time $t$. |
| $u_{i,t}^{DIS}$ | Discharging state variable of storage unit $i$ at time $t$. |
| $u_{i,t}^{CHG}$ | Charging 0–1 state variable of storage unit $i$ at time $t$. |
| $p_{i,t}$ | Output of unit $i$ during normal-load generation at time $t$ (MW). |
| $p_{i,b,t}$ | Output of unit $i$ of segment $b$ during normal-load generation at time $t$ (MW). |
| $p_{i,t}^D$ | Output of unit $i$ during low-load generation without FCS at time $t$ (MW). |
| $p_{i,t}^{DC}$ | Output of unit $i$ during low-load generation with FCS at time $t$ (MW). |
| $p_{i,t}^N$ | Normal-load generation output of unit $i$ at time $t$ (MW). |
| $p_{i,b,t}^D$ | Output of unit $i$ of segment $b$ during low-load generation without FCS at time $t$ (MW). |
| $p_{i,b,t}^{DC}$ | Output of unit $i$ of segment $b$ during low-load generation with FCS at time $t$ (MW). |
| $p_{i,t}^{DIS}$ | Discharging power of storage unit $i$ at time $t$ (MW). |
| $p_{i,t}^{CHG}$ | Charging power of storage unit $i$ at time $t$ (MW). |
| $r_{i,t}^U$ | Upward reserve capacities of generator $i$ at time $t$ (MW). |
| $r_{i,t}^D$ | Downward reserve capacities of generator $i$ at time $t$ (MW). |
| $f_{i,t}$ | Segmented linearized generation cost of unit $i$ at time $t$ ($). |
| $f_{i,t}^D$ | Cost of unit $i$ at time $t$ during low-load generation without FCS ($). |
| $f_{i,t}^N$ | Normal-load generation cost of unit $i$ at time $t$ ($). |
| $f_{i,t}^{DC}$ | Cost of unit $i$ at time $t$ during low-load generation with FCS ($). |
| $p_{j,t}$ | Power of load $j$ at time $t$ (MW). |
| $y_{i,t}$ | Start-up 0–1 variable of generator $i$ at time $t$. |
| $z_{i,t}$ | Shutdown 0–1 status variable of generator $i$ at time $t$. |

## Appendix A. Six-Buses System Information

**Table A1.** Data of generators and renewable plant.

| Index | Bus | Type | Capacity/MW |
|---|---|---|---|
| 1 | A | Coal-fired generator | 300 |
| 2 | A | Coal-fired generator | 300 |
| 3 | A | Coal-fired generator | 200 |
| 4 | A | Coal-fired generator | 300 |
| 5 | B | Coal-fired generator | 300 |
| 6 | D | Coal-fired generator | 100 |
| 7 | D | Coal-fired generator | 300 |
| 8 | B | PV | 100 |
| 9 | B | Wind | 700 |

**Table A2.** Energy storage data.

| Bus | Maximum Capacity (MW) | Maximum Energy (MWh) | Charging Efficiency | Discharge Efficiency |
|---|---|---|---|---|
| B | 100 | 200 | 0.922 | 0.922 |

**Table A3.** Marginal cost during low-load generation without FCS.

| Cost Segment Index | Generator 2 Capacity Segment (MW) | Generator 2 Cost Segment (RMB) | Generator 4 Capacity Segment (MW) | Generator 4 Cost Segment (RMB) |
|---|---|---|---|---|
| 1 | 9 | 10 | 9 | 15 |
| 2 | 9 | 20 | 9 | 25 |
| 3 | 9 | 30 | 9 | 35 |
| 4 | 9 | 40 | 9 | 45 |
| 5 | 9 | 50 | 9 | 55 |
| 6 | 9 | 60 | 9 | 65 |
| 7 | 9 | 70 | 9 | 75 |

**Table A4.** Marginal cost during low-load generation with FCS.

| Cost Segment Index | Generator 2 Capacity Segment (MW) | Generator 2 Cost Segment (RMB) | Generator 4 Capacity Segment (MW) | Generator 4 Cost Segment (RMB) |
|---|---|---|---|---|
| 1 | 9 | 80 | 9 | 85 |
| 2 | 9 | 90 | 9 | 95 |
| 3 | 9 | 100 | 9 | 105 |

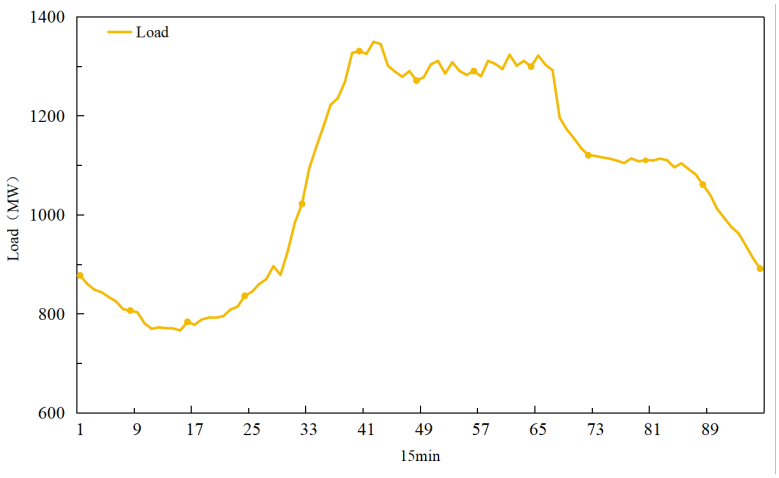



**Figure A1.** Typical load profile.

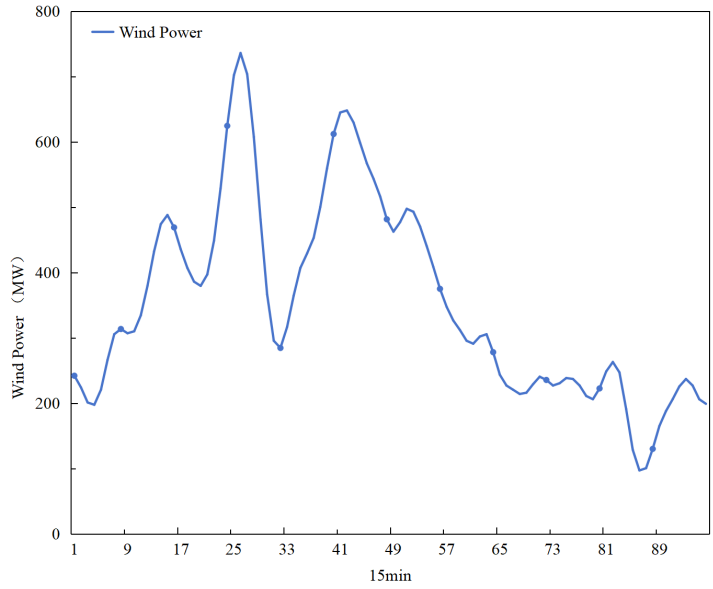



**Figure A2.** Typical wind generation profile.

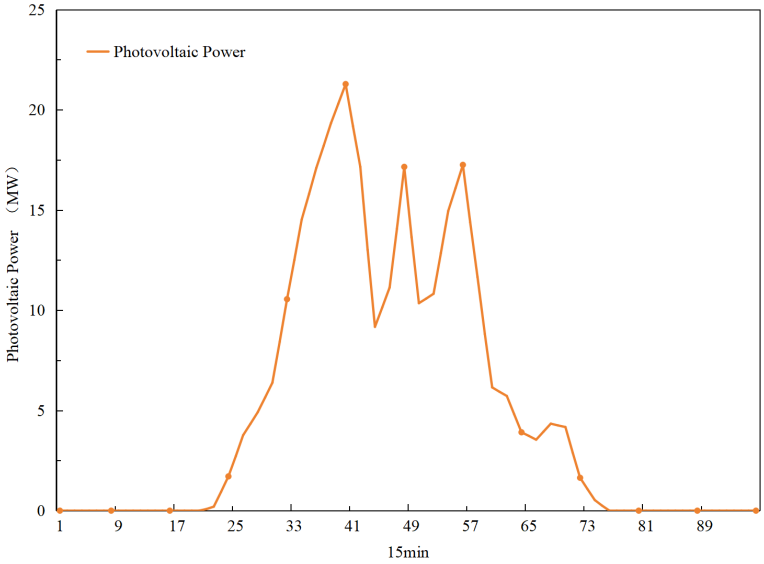



**Figure A3.** Typical PV generation profile.

## References


1. Zhao, J.; Zheng, T.; Litvinov, E. A Unified Framework for Defining and Measuring Flexibility in Power System. *IEEE Trans. Power Syst.* **2016**, *31*, 339–347. [CrossRef]
2. Tsiaras, E.; Andreosatou, Z.; Kouveli, A.; Tampekis, S.; Coutelieris, F.A. Off-Grid Methodology for Sustainable Electricity in Medium-Sized Settlements: The Case of Nisyros Island. *Clean Technol.* **2025**, *7*, 16. [CrossRef]
3. Lu, J.; Qiu, C.; Zhang, G.; Lei, G.; Zhu, J. Seizing Unconventional Arbitrage Opportunities in Virtual Power Plants: A Profitable and Flexible Recruitment Approach. *Appl. Energy* **2024**, *358*, 122628. [CrossRef]
4. Na, C.; Pan, H.; Zhu, Y.; Yuan, J.; Ding, L.; Yu, J. The Flexible Operation of Coal Power and Its Renewable Integration Potential in China. *Sustainability* **2019**, *11*, 4424. [CrossRef]
5. Wei, H.; Lu, Y.; Yang, Y.; Wu, Y.; Zheng, K.; Li, L. Research on Thermal Adaptability of Flexible Operation in Different Types of Coal-Fired Power Units. *Energies* **2024**, *17*, 2185. [CrossRef]
6. Ye, H.; Xie, L.; Deng, J.; Wang, Z.; Bao, H. Low-Carbon Optimal Dispatch of Wind–Thermal Coordination Considering Carbon Trading Mechanism. *Acta Energiae Solaris Sin.* **2023**, *44*, 106–112. [CrossRef]
7. Yang, B.; Cao, X.; Cai, Z.; Yang, T.; Chen, D.; Gao, X.; Zhang, J. Unit Commitment Comprehensive Optimal Model Considering the Cost of Wind Power Curtailment and Deep Peak Regulation of Thermal Unit. *IEEE Access* **2020**, *8*, 71318–71325. [CrossRef]
8. Wu, W.; Zhu, J.; Chen, Y.; Luo, T.; Shi, P.; Guo, W.; Shi, P.; Jiang, C. Modified Shapley Value-Based Profit Allocation Method for Wind Power Accommodation and Deep Peak Regulation of Thermal Power. *IEEE Trans. Ind. Appl.* **2023**, *59*, 276–288. [CrossRef]
9. Lin, L.; Tian, X. Economic Dispatch and Benefit Analysis for Power Systems Based on Graded Deep Peak Shaving of Thermal Power Units. *Power Syst. Technol.* **2017**, *41*, 2255–2262.
10. Teng, M.; Chen, C.; Zhao, Y.; Zhong, J.; Geng, J.; Lü, J.; Bie, C. Day-Ahead Robust Distributed Optimization for Power Systems with Uncertain Wind Integration Considering Deep Peak Regulation and Energy Storage. *Power Syst. Technol.* **2024**, *48*, 3122–3132. [CrossRef]
11. Meng, Y.; Cao, Y.; Li, J.; Liu, C.; Li, J.; Wang, Q.; Cai, G.; Zhao, Q.; Liu, Y.; Meng, X.; et al. The Real Cost of Deep Peak Shaving for Renewable Energy Accommodation in Coal-Fired Power Plants: Calculation Framework and Case Study in China. *J. Clean. Prod.* **2022**, *367*, 132913. [CrossRef]
12. Zhang, Q.; Dong, J.; Chen, H.; Feng, F.; Xu, G.; Wang, X.; Liu, T. Dynamic Characteristics and Economic Analysis of a Coal-Fired Power Plant Integrated with Molten Salt Thermal Energy Storage for Improving Peaking Capacity. *Energy* **2024**, *290*, 130132. [CrossRef]
13. Xing, C.; Xiao, J.; Xi, X.; Li, J.; Li, P.; Zhang, S. Two-Layer Optimal Scheduling and Economic Analysis of Composite Energy Storage with Thermal Power Deep Regulation Considering Uncertainty of Source and Load. *Energies* **2024**, *17*, 4909. [CrossRef]
14. Wang, G.; You, D.; Lou, S.; Zhang, Z.; Dai, L. Economic Valuation of Low-Load Operation with Auxiliary Firing of Coal-Fired Units. *Energies* **2017**, *10*, 1317. [CrossRef]
15. Pang, Y.; Chi, Y.; Tian, B. Economic Evaluation of Flexible Transformation in Coal-Fired Power Plants with Multi Price Links. *J. Clean. Prod.* **2023**, *402*, 136851. [CrossRef]
16. Zheng, K.; Xu, F.; Xue, N.; Li, H.; Zhao, J.; Wang, S. Trading Mechanism and Clearing Method of Day-Ahead and in-Day Deep Peak Shaving Markets. In Proceedings of the 2023 3rd International Conferance of Energy, Power and Electrical Engineering (EPEE), Wuhan, China, 15–17 September 2023; pp. 1476–1482.
17. Shi, Y.; Li, Y.; Zhou, Y.; Xu, R.; Feng, D.; Yan, Z.; Fang, C. Optimal Scheduling for Power System Peak Load Regulation Considering Short-Time Startup and Shutdown Operations of Thermal Power Unit. *Int. J. Electr. Power Energy Syst.* **2021**, *131*, 107089. [CrossRef]
18. Xiang, H.; Yao, X.; Jiang, W.; Kang, J.; Zhu, S.; Zhu, X.; Song, Z. Hydro-Thermal Joint Optimization of Multi-Objective Unit Commitment Considering Negative Peak Load Regulation Ability. In Proceedings of the 2018 International Conference on Power System Technology (POWERCON), Guangzhou, China, 6–8 November 2018; pp. 1202–1207. [CrossRef]
19. Jiang, Z.; Wang, J.; Xiao, Y.; Yan, X.; Liu, Q.; Ye, L. Market Clearing Model and Pricing Method for Combined Energy and Deep Peak Regulation Markets Based on Two-Stage Stochastic Optimization. *Power Syst. Technol.* **2023**, *47*, 3597–3613. [CrossRef]
20. Ding, Q.; Ren, Y.; Hu, X.; Zou, P.; Yan, Z.; Li, M.; Cai, Z.; Xue, Y. Design and Practice of the Joint Optimization Mechanism of Shanxi Electricity Spot and Deep Peak Regulation Market. *Power Syst. Technol.* **2021**, *45*, 2219–2228. [CrossRef]
21. Li, J.; Chen, Y.; Liu, S.; Zhang, X.; Ma, Z.; Zhong, H. Design of Day-Ahead Electricity Market Mechanism Considering Deep Peak Regulation. *Autom. Electr. Power Syst.* **2019**, *43*, 9–15+78.
22. Qi, L.; Chen, B.; Jiang, P.; Zhao, R.; Gao, X. Cost and Benefit Analysis of Peak Regulation Ancillary Services Provided by Coal-Fired Units. *Electr. Power Big Data* **2019**, *22*, 23–29. [CrossRef]
23. Wang, J.; Huo, J.; Zhang, S.; Teng, Y.; Li, L.; Han, T. Flexibility Transformation Decision-Making Evaluation of Coal-Fired Thermal Power Units Deep Peak Shaving in China. *Sustainability* **2021**, *13*, 1882. [CrossRef]

24. Wang, S. Peak Shaving Market-Oriented Bidding Model of Coal-Fired Power Considering Deep Peak Regulation Cost. M.S. Thesis, Huazhong University of Science and Technology, Wuhan, China, 2020.
25. IBM Corporation. *Introducing IBM ILOG CPLEX Optimization Studio 22.1.1*; IBM: Armonk, NY, USA, 2022. Available online: https://www.ibm.com/docs/en/icos/22.1.1?topic=documentation-introducing-ilog-cplex-optimization-studio-2211 (accessed on 24 August 2025).

**Disclaimer/Publisher's Note:** The statements, opinions and data contained in all publications are solely those of the individual author(s) and contributor(s) and not of MDPI and/or the editor(s). MDPI and/or the editor(s) disclaim responsibility for any injury to people or property resulting from any ideas, methods, instructions or products referred to in the content.